ARTICLE

CO$_2$-Responsive Smart Foams Stabilized by an Extremely Rigid Bio-Based Surfactant

Weishan Tang, Xin Feng, Caiyun Lin and Xiaoping Rao[*]

College of Chemical Engineering, Huaqiao University, Xiamen, 361021, China

[*]Corresponding Author: Xiaoping Rao. Email: raoxp@hqu.edu.cn

ABSTRACT

Environment friendly and intelligent surfactants have attracted great attention in recent years. A bio-based CO$_2$ responsive surfactant rosin acid dimaleimide choline (R-BMI-C) with an extremely rigid skeleton was prepared using rosin and choline as raw materials by Diels-Alder addition reaction and acid-base neutralization reactions. Its structure was confirmed by IR and ^{1}H NMR spectra. The foams' properties of R-BMI-C could be adjusted by bubbling CO$_2$/N$_2$ to change the structure of the surfactant. At pH 10.4, R-BMI-C forms an unstable foam with a half-life of 1.5 h. When the pH was reduced to 7.4 by bubbling CO$_2$, R-BMI-C forms an extremely stable foam with a half-life of 336 h. The surfactant R-BMI-C changed from bola type to conventional type when bubbling CO$_2$. And the internal aggregation structure of R-BMI-C aqueous solution changed from spherical micelles to laminar micelles according to the cryogenic-transmission electron microscope. We know that the lamellar structure tends to adsorb at the air/water interface or is trapped in the foam film, which slows down the foam coarsening and agglomeration process, resulting in a significant increase in foam stability. R-BMI-C could be used in oil extraction, fire-fighting and chemical decontamination due to its excellent foaming, stabilization and defoaming properties.

KEYWORDS

Rosin; bio-based; surfactant; CO$_2$-responsive; foams

1 Introduction

Foams are a dispersion of an insoluble gas in a liquid or solid, which has the excellent properties of light mass, large specific surface area and high mobility [1,2]. Therefore, foams are used in numerous industrial processes, such as oil recovery, mineral flotation, cosmetics, fire-fighting and chemical decontamination [3–6]. As we all know, foams are sub-stable systems where the dispersed gas is wrapped in a liquid film. Over time gas transfer between foams occurs, the average foams particle size increases and the liquid film breaks down [7]. To effectively stabilize foams, stabilizers such as proteins, surfactants, polymers and nanoparticles are usually added [1,8,9]. Stabilizers stabilize foam by slowing down the three foam destabilization mechanisms of foams' drainage, coarsening and coalescence [10,11].

However, in some industrial production such as wastewater treatment and material recovery, the presence of stable foams is destructive and needs to be defoamed promptly at the end of use [2]. The most common method currently used is the addition of a defoamer, but the defoamer is difficult to separate from the components and causes contamination of the original system. And its addition hinders

the product from foaming again, making it impossible to be used twice [12–14]. To solve this problem, stimuli-responsive surfactants have attracted a lot of attention from researchers [15]. Through certain triggering mechanisms, such as pH [3], temperature [16,17], CO_2/N_2 [18–20] and light [21], structural changes are induced in the surfactant molecules in solution. The reversible transition between "surface-active" and "non-surface active" surfactant results in responsive foams that can switch between stable and unstable states. In fact, pH-sensitive surfactants generally contain ionizable organic groups such as carboxyl, phenylhydroxyl and amino groups [3]. Their solubility or ionization state changes with the pH of the solution, leading to a shift in their macroscopic properties. Usually, researchers have used the addition of acids or bases to change the pH of the solution. However, they generate by-products that disturb the original system. CO_2, being an environmentally friendly gas, does not accumulate in the system when used as a trigger. After bubbling CO_2 into the solution, it forms carbonates with water and lowers the pH of the solution. The surfactant molecules in the solution are protonated. Since the carbonate is very unstable, the original system can be restored to its initial state by simply passing N_2 under heated conditions.

Most surfactants are currently produced from petrochemical resources, which is not conducive to green and sustainable development. The use of natural products as raw materials instead of traditional petroleum resources to synthesize green surfactants has become an industry trend. Rosin is a forest resource with abundant production and is one of the main raw materials for the preparation of green surfactants [7,22]. Its unique tricyclic diterpene rigid skeleton structure can be arranged more regularly at the gas/liquid interface, increasing the strength of the interfacial film and forming stable foams [23–25]. Lei et al. [12] synthesized an azo-benzene surfactants from dehydrofirmanoic acid, which can be adjusted to the trans-cis isomerization of the azo-benzene moiety using UV light. Zhai et al. [7] prepared a pH-responsive surfactant from rosin, which can adjust the pH of the solution by adding acid and base to regulate the foaming performance of the surfactant. However, the structural modification of surfactants containing rigid structure and their conformational relationships are still under-studied.

In this article, we synthesized an extremely rigid rosin-based amphiphile surfactant rosin acid dimaleimide choline (R-BMI-C). By Diels-Alder addition and acid-base neutralization reactions, we obtained a large rigid skeleton and introduced CO_2/N_2 responsive groups. The strongly responsive surface activity and self-organized system were realized. In addition, the CO_2 responsive surfactants formation was constructed by forming carboxylic acid choline salt expands the controllable range of surfactants.

2 Experimental Section

2.1 Sample Preparation and Characterization

Abietic Acid (purity >95%) was purchased from Westech Chemical Co. Ltd., Guangzhou, China. N, N'-(4,4'-Methylenediphenylene) dimaleimide (BMI), p-Toluenesulfonic acid and choline (44% weight in water) were obtained from Maclean's Chemistry Company, Shanghai, China. Acetic acid (AR), acetone (AR) and petroleum ether (AR) were purchased from Sinopharm Chemical Reagent Co. Ltd., Shanghai, China. All reagents were used as received.

Fourier transform infrared (FT-IR) spectra were recorded by Thermo Scientific Nicolet and tested in the wavenumber range of 400~4000 cm^{-1}. ^{1}H NMR was measured by 500 MHz Nuclear Magnetic Resonance Spectroscopy using deuterated dimethyl sulfoxide as the solvent.

2.2 Synthetic Methods

2.2.1 Synthesis of Rosin Acid Dimaleimide (R-BMI)

10 g of Abietic Acid and 4.3 g of N, N'-(4,4'-Methylene-diphenyl) bismaleimide were dissolved in 30 mL of acetic acid and 0.46 g of p-toluenesulfonic acid was added as catalyst. The mixture was stirred at 120°C for 15 h. After cooling to room temperature, the crystalline R-BMI was obtained by filtration.

The crystals were recrystallized using acetone as solvent. Finally, the resulting solid was dried under vacuum at 70°C for 12 h.

2.2.2 Synthesis of Rosin Acid Dimaleimide Choline (R-BMI-C)

Firstly, choline solution with a concentration of 0.02 mM was prepared in ultrapure water, and then the choline solution was mixed with R-BMI in the ratio of molar ratio $R = \frac{n_{choline}}{n_{rosin\ acid\ dimaleimide}} = 2.4$, and the reaction was carried out at a temperature of 75°C for 1 h. When the reaction solution was cooled to room temperature at the end, it was extracted with petroleum ether three times and freeze-dried for 12 h to obtain R-BMI-C. The synthetic route of R-BMI-C was shown in Fig. 1.
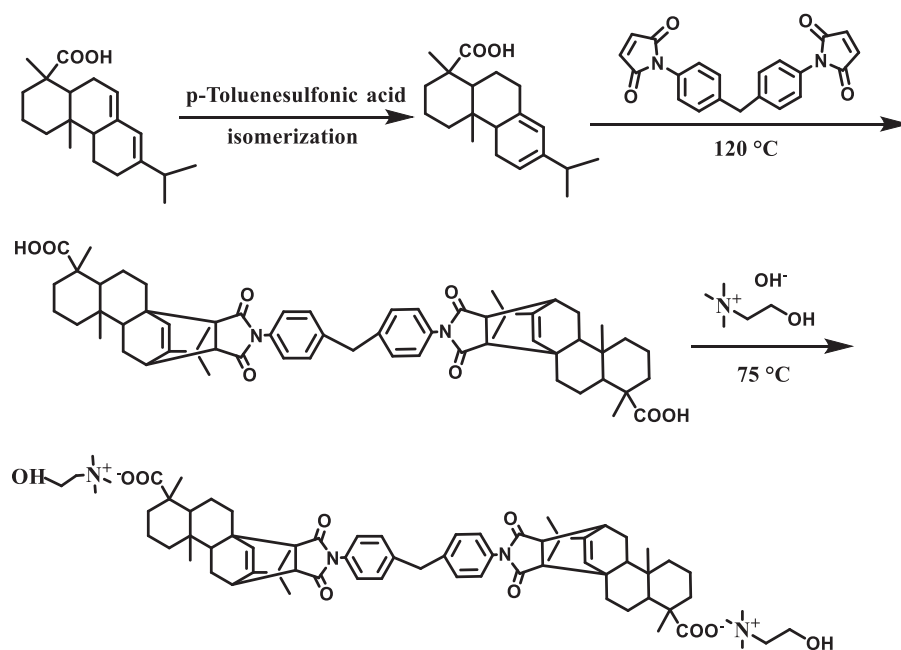

Figure 1: Synthesis of R-BMI-C

2.3 CO₂/N₂ Responsive

Aqueous solutions of surfactants of different concentrations were bubbled with CO_2 until the solutions obtained the desired pH. CO_2 can be removed by passing N_2 into the solution at 65°C for 1–2 h.

2.4 pH Measurement

To confirm the responsiveness of the rosin-based amphiphile surfactant, the pH of the surfactant solution (Sigma pH test pen) was measured under the conditions of alternate passage and removal of CO_2. The pH of each sample was measured three times and the average value was taken.

2.5 Surface Tension Measurement

The surface tension of R-BMI-C was measured by the SDC-100S contact angle meter. The dynamic surface tension of the R-BMI-C aqueous solution at different concentrations and pH were determined by the suspension drop method. R-BMI-C was prepared as two series concentration surfactant solutions, and the pH of prepared surfactant solutions were adjusted to10.4 and 7.4 by bubbling CO_2, respectively. All samples were performed at room temperature, and each sample was tested three times and averaged, with negligible differences between measurements.

2.6 Foaming and Foam Stabilization

Add 4 mL of surfactant solutions of different concentrations at different pH values to a 10 mL stoppered measuring cylinder, respectively. The surfactant solutions were shaken vigorously by hand for 30 s. All foams were prepared by the same operator to avoid excessive errors. To characterize the foaming properties of the surfactant solutions, we recorded the volume of foams formed. And the foams' stabilization was determined by recording the change in foams volume with time.

2.7 Fluorescence Microscope Observation

The morphology of the foams was obtained by a ZYF-2000E inverted fluorescence microscope (Shanghai Zhaoyi Photoelectric Technology Co., Ltd.). The microscope is equipped with a color camera to take digital images (4632 × 3488). The foams with different pH were prepared according to the method in 2.6 and tested after standing for 5 min. A drop of foam was placed on a clean slide (24 × 60 mm) and covered with another slide (18 × 18 mm), and then the micrographs were recorded.

2.8 Cryogenic-Transmission Electron Microscope (Cryo-TEM)

The microscopic morphology of the rosin-based surfactant solution was observed by Cryo-TEM. 5 μL of the solution to be measured was added dropwise to the copper mesh using a pipette, then the copper mesh was quickly placed in liquid propane, and the prepared samples were placed in liquid nitrogen for storage. The frozen sample rod was Gatan 626, tested by applying a JEOL JEM-1400 transmission electron microscope, and the images were collected and stored by Gatan 831 CCD.

3 Results and Discussion

3.1 Synthesis and Structure Characterization of R-BMI-C

The structure of rosin acid contains two reactive centers, double bonds and carboxyl group, which are easy to be chemically modified. In this study, the rigid structure rosin acid was used as the raw material, and with the intervention of p-toluenesulfonic acid, the rosin acid underwent isomerization to generate the more reactive levopimaric acid. The conjugated double bonds of levopimaric acid underwent Diels-Alder addition reaction with the diolefins hydrocarbon of bismaleimide to produce rosin acid bismaleimide. Finally, the desired product R-BMI-C was obtained by a simple acid-base neutralization reaction of rosin acid bismaleimide with choline.

The chemical structures of R-BMI-C were characterized by FT-IR and ^{1}H-NMR. FT-IR spectra of R-BMI and R-BMI-C were shown in Fig. 2. ^{1}H NMR spectrum of R-BMI and R-BMI-C were shown in Figs. 3 and 4, respectively. It indicates that the intermediate product R-BMI and the target product R-BMI-C have been successfully synthesized.

The absorption peaks at 3444.73 cm^{-1} are stretching vibrational peaks of hydroxyl groups (-OH), 2935.13 and 2868.60 cm^{-1} for methyl and methylene (CH$_3$-, -CH$_2$-), 1770.82 cm^{-1} for amide (-CO-N-OC-), and 1698.98 cm^{-1} for carboxylic acid (-COOH). After the reaction with choline, a new stretching vibration peak of carboxylic acid ion (-COO$^-$) appeared at 1560.07 cm^{-1}, and it can be inferred that the target product R-BMI-C has been synthesized.

^{1}H NMR (500 MHz, DMSO) δ 7.30 (m, 4H, C3-4H), 6.97 (m, 4H, C2-4H), 5.50 (s, 2H, C6-2H), 3.98 (s, 4H, C1-4H), 3.43 (m, 2H, C5-2H), 2.70 (d, 2H, C4-2H), 2.43-2.40 (m, 4H, C9-2H, C20-2H), 1.73-1.36 (m, 26H, C14-4H, C10-4H, C11-4H, C15-4H, C16-4H, C19-4H, C12-2H, C13-6H), 1.05 (s, 2H, C18-2H), 0.94-0.91 (m, 18H, C7-6H, C8-6H, C17-6H).
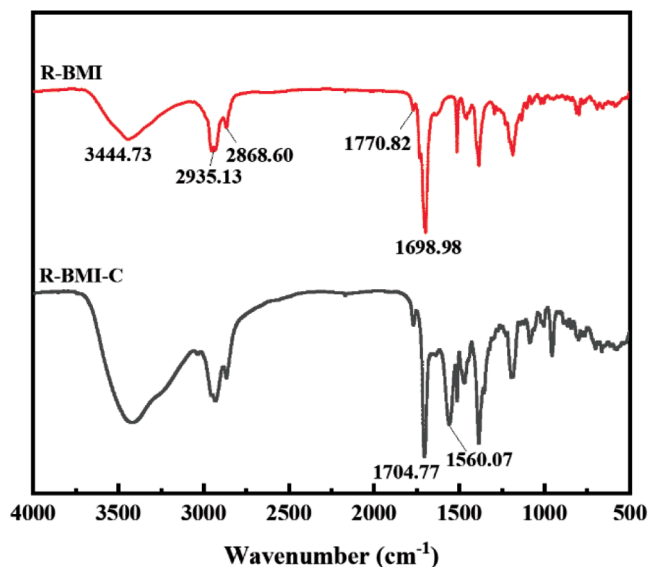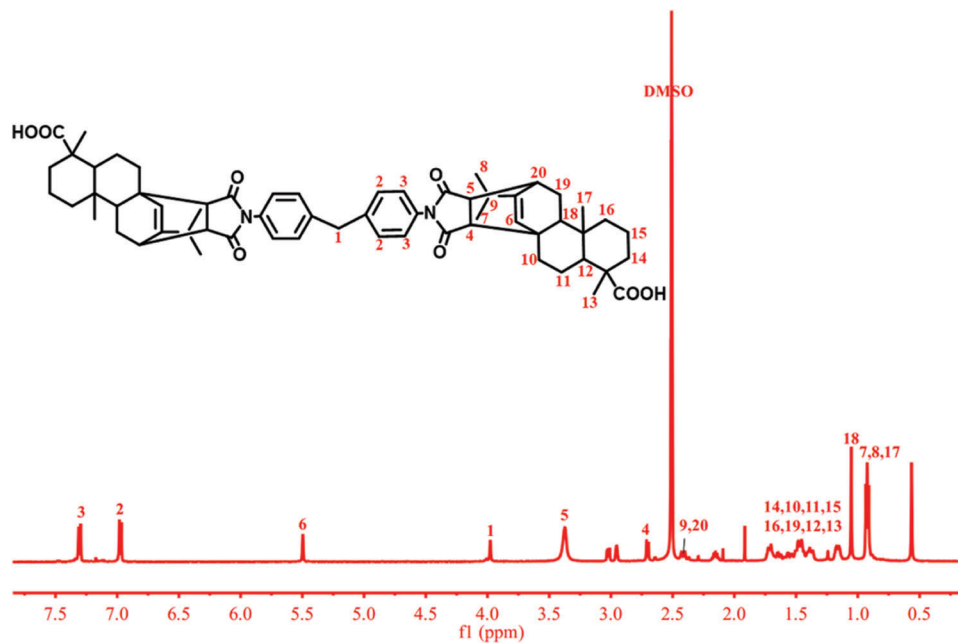
Figure 2: FT-IR spectra of R-BMI and R-BMI-C

Figure 3: ^{1}H-NMR spectrum of R-BMI

^{1}H NMR (500 MHz, DMSO) δ 7.30 (m, 4H, C3-4H), 6.97 (m, 4H, C2-4H), 5.50 (s, 2H, C6-2H), 3.98 (s, 4H, C1-4H), 3.43 (m, 2H, C5-2H), 3.13 (s, 18H, C21-18H), 3.09 (s, 4H, C22-4H), 2.64 (d, 2H, C4-2H), 2.43-2.40 (m, 4H, C9-2H, C20-2H), 1.81-1.15 (m, 26H, C14-4H, C23-4H, C10-4H, C11-4H, C15-4H, C16-4H, C19-4H, C12-2H, C13-6H), 1.05-0.83 (m, 22H, C18-2H, C24-2H, C7-6H, C8-6H, C17-6H).
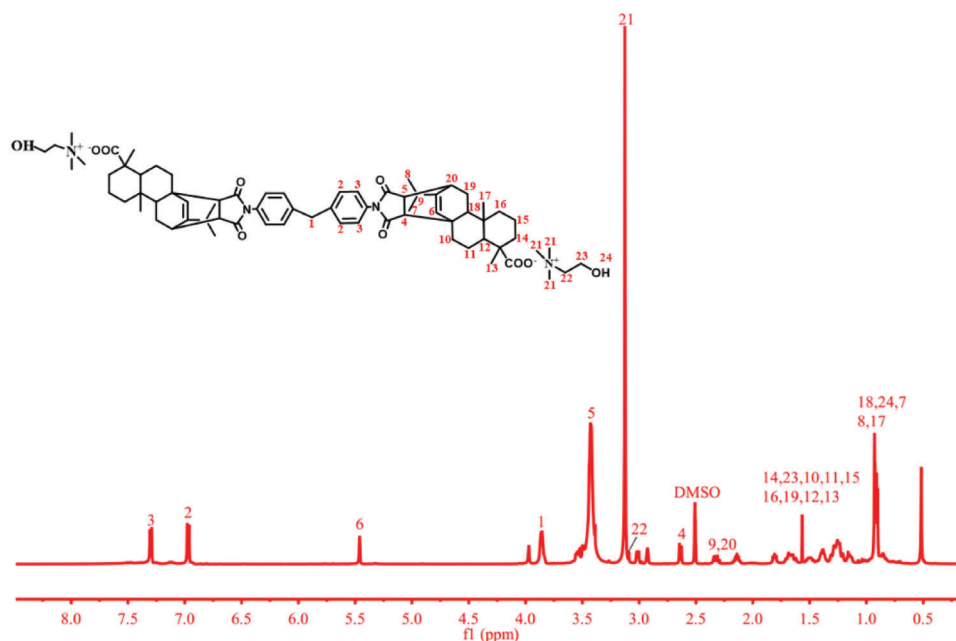
Figure 4: ^{1}H-NMR spectrum of R-BMI-C

The number of hydrogens of the synthesized product was the same as that of the target product, and the chemical shifts of the characteristic hydrogens were similar to those of the target product. It showed that the intermediate product R-BMI and the target product R-BMI-C were successfully synthesized.

3.2 Determination of Ionization Equilibrium Constants

R-BMI-C (1 g/L) was dissolved in 0.1 M NaOH solution and titrated with 0.1 M HCl solution. Determine the pH at different HCl volumes and make an acid-base titration curve with pH as the y-axis and HCl volume as the x-axis.

Fig. 5 shows the acid-base titration curve of R-BMI-C. Initially, the added HCl reacts with the NaOH in the solution in a neutralization reaction, at which time the pH of the solution slowly decreases. When NaOH is finished being reacted, the pH drops faster. When the pH of the solution is 10.17, the pH drop slows down. This indicates that part of the -COO$^-$ of R-BMI-C starts to combine with H$^+$ to convert to -COOH. At this time, R-BMI-C transforms from a bola-type surfactant containing a hydrophobic backbone with two hydrophilic groups to a conventional-type surfactant with a single head and a single tail. As can be seen from the figure, when the pH was further reduced to 7.42, the -COO$^-$ at the other end of R-BMI-C also started to combine with H$^+$ to convert to -COOH. Until the pH of the solution was reduced to 5.39, the solution R-BMI-C was completely acidified. From the above results, the two ionization equilibrium constants of R-BMI-C are 10.17 and 7.42, respectively.

3.3 The Transmittance of R-BMI-C Aqueous Solution

The transmittance of R-BMI-C was measured using a UV 2450 UV spectrophotometer with a test wavelength of 200–800 nm. The aqueous solution of R-BMI-C was added to a quartz cell with a 1 cm optical path length at 25°C, with ultrapure water as the background.
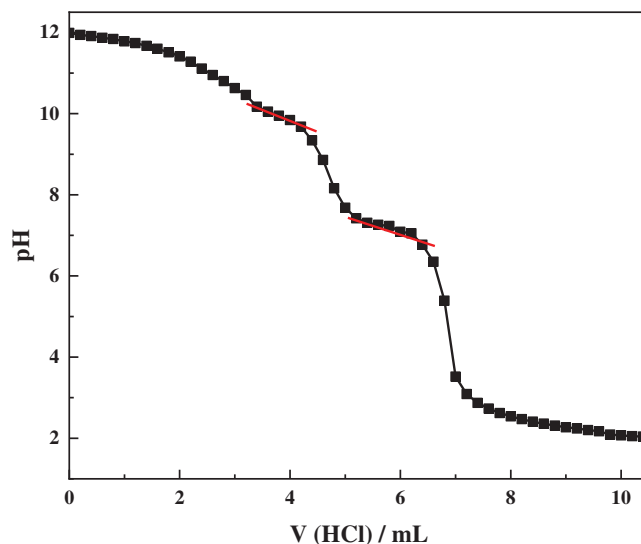
Figure 5: Variation curve of pH with the volume of HCl in the R-BMI-C aqueous solution

First, we bubbled CO_2 into the R-BMI-C aqueous solution (2 mM) to regulate the pH of the surfactant solution. The transmittance was also measured to determine the dissolution of R-BMI-C at different pH values, and the results are given in Fig. 6. The transmittance of R-BMI-C aqueous exceeded 99.17% when the pH was large than 10.3, at which time R-BMI-C was completely dissolved in water. The pH value of the solution decreased by bubbling CO_2 into the aqueous surfactant solution. The transmittance decreased with the decrease of pH value, and the transmittance was 2.38% when the pH value decreased to 6.3. It indicates that lots of R-BMI-C precipitated from the solution. During the bubbling of CO_2, H^+ was produced in the solution and R-BMI-C was protonated. When the pH was in the range of 6.3 to 10.3, both protonated (-COOH) and deprotonated (-COO$^-$) forms of R-BMI-C coexist in the solution. And at pH less than 6.3, R-BMI-C is completely protonated and converted to its acid form. Therefore, the pH of the aqueous R-BMI-C solution was adjusted to greater than 6.3.
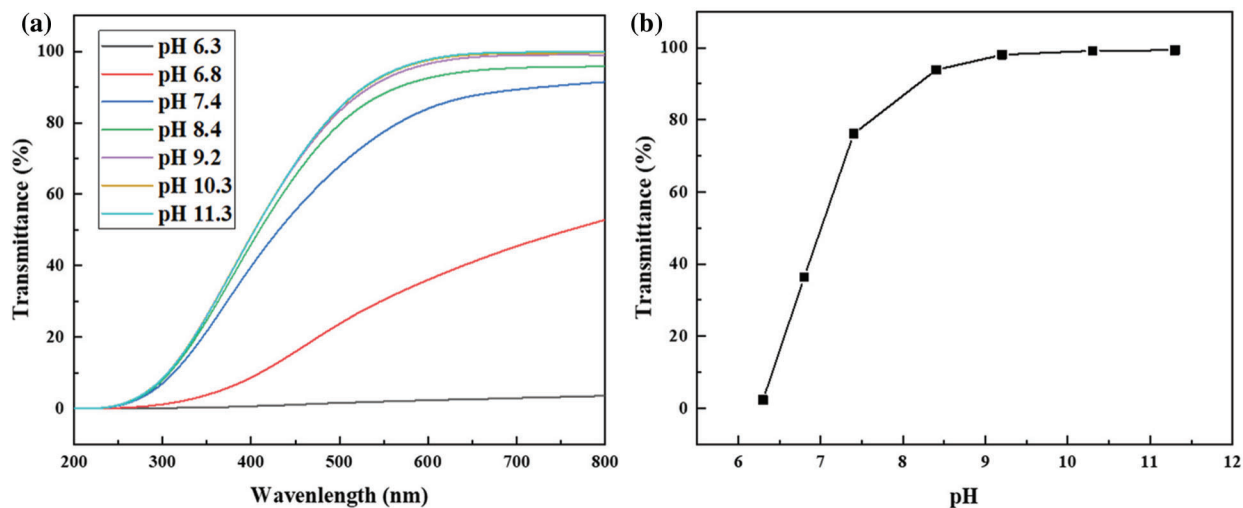

Figure 6: (a) Variation of transmittance of R-BMI-C with wavelength at different pH values; (b) transmittance of R-BMI-C at different pH values at 600 nm

3.4 Surface Tension and Critical Micelle Concentration of R-BMI-C

R-BMI-C has an excellent ability to reduce surface tension. The surface tension of R-BMI-C at pH 7.4 and pH 10.4 is shown in Fig. 7. The surface tension of the R-BMI-C aqueous solution showed two inflection points with increasing concentration. This is consistent with the properties of bola-type surfactants, which contain a hydrophobic backbone with two hydrophilic groups at both ends [26]. The second inflection point was the critical micelle concentration (cmc) [27], and the value of the cmc was 0.55 mM. When the pH was reduced to 7.4, some of the carboxylate ions of R-BMI-C were converted to carboxyl groups, and the transformation of the surfactant from bola type to conventional type was achieved. At this time, the cmc value of R-BMI-C was 0.09 mM, exhibiting strong aggregation ability. In the intervention of CO_2, some of the carboxylate ions of the surfactant were protonated (-COOH). The solution pH was changed and the cmc was also changed about 6-fold, exhibiting significant aggregation differences before and after the response. Sanchez-Fernandez et al. reported phosphocholine and sulfobetaine surfactants [28]. They both had cmc values of about 1 mM, when the sulfobetaine surfactant could reduce the surface tension to 32.79 mN·m^{-1}, exhibiting excellent surface tension reduction. The fully rigid backbone of R-BMI-C has relatively fixed positions of carbon atoms, which cannot resist structural changes caused by environmental changes by twisting or bending like flexible chains. This property allows it to maximize the property changes caused by molecular structure changes triggered by external stimuli [12]. However, the large rigid structure of R-BMI-C hinders its ability to reduce surface tension. At pH 10.4 and pH 7.4, the surface tensions of R-BMI-C at cmc were 42.79 and 47.83 mN·m^{-1}, respectively, which were significantly higher than those of surfactants containing flexible chains in general. The surface tensions were significantly higher than those of the general surfactants containing flexible chains. It shows that R-BMI-C is more capable of aggregation but less capable of reducing surface tension.
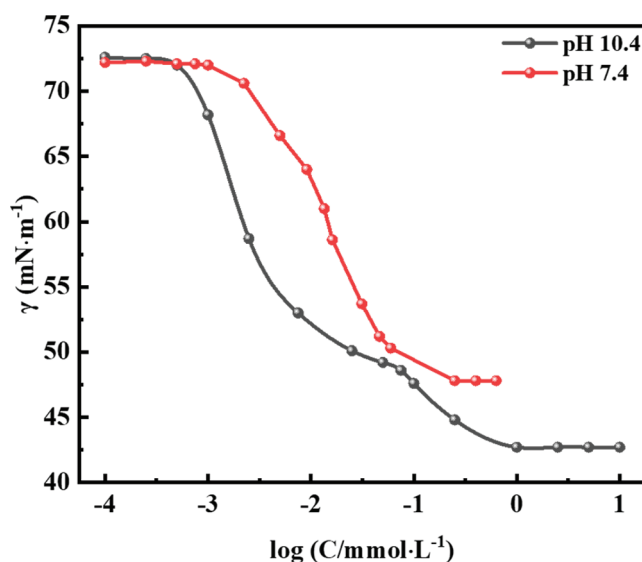

Figure 7: Surface tension as a function of concentration for R-BMI-C aqueous solutions at pH 7.4 and pH 10.4

3.5 The Effect of Concentration on Foams

To evaluate the foams' performance of R-BMI-C, we bubbled CO_2 into R-BMI-C aqueous solution to adjust its pH to 7.4 and studied the foam produced by R-BMI-C aqueous solution at this time. Firstly, we prepared a series of aqueous solutions of R-BMI-C with a concentration gradient. Stable foams were

formed by vigorous shaking for 30 s. As shown in Fig. 8a, the foams volumes were 2.6, 4.0, 5.2 and 6.2 mL for concentrations of 0.1, 0.5, 1 and 2 mM, respectively. The initial volume of foams increased with the increase of R-BMI-C aqueous solution concentration. The stability of the foams was commonly judged by their half-life time, which is the time required to reduce the volume of the foam to half of the initial volume. Fig. 8b records the variation of the volume of the foam formed by the R-BMI-C aqueous solution at each concentration with time. This resulted in foams half-lives of 3, 196, 310, and 336 h for R-BMI-C aqueous solutions with concentrations of 0.1, 0.5, 1, and 2 mM, respectively. As far as we know, Lei et al. [12] reported a half-life of 976 min for almost completely rigid R-AZO-Na at a concentration of 4 mM. Zhai et al. [7] reported a half-life of 2145 min for the bola-type surfactant Na-MPA-AZO-Na at 2 mM. In conclusion, the completely rigid surfactant R-BMI-C has excellent foams stabilization properties. This is attributed to its large rigid backbone structure, which is more regularly arranged at the gas-liquid interface than the flexible hydrophobic chains. Thus, increasing the strength of the interfacial film and forming a more stable foam.
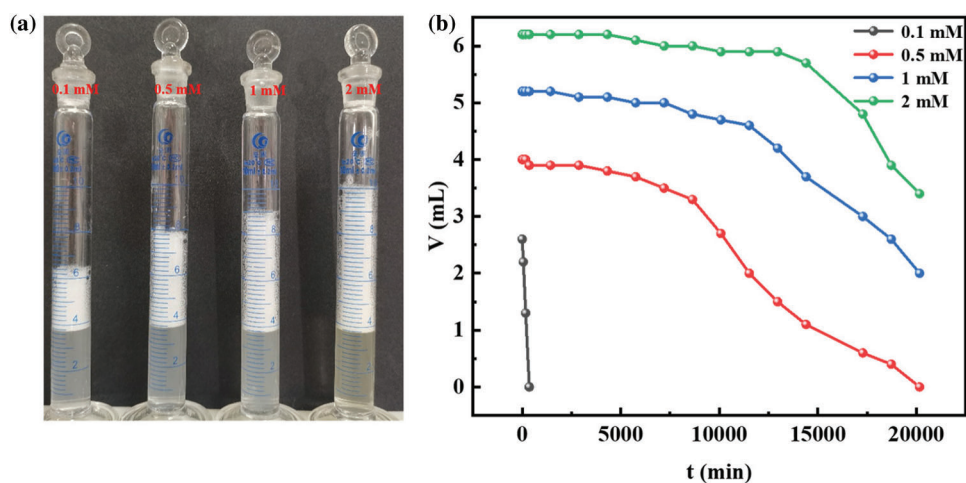

Figure 8: (a) Digital photographs of aqueous foams (b) Variation of foams volume by R-BMI-C aqueous solutions with concentrations of 0.1, 0.5, 1, and 2 mM at pH 7.4

In this paper, we used the shaking hand method to characterize the foaming properties of the surfactant solutions. Each set of experiments was repeated three times. Even though the experiments were operated by the same person, there were still errors. The error bars of foaming and foam stabilization tests are shown in Fig. 9.

3.6 CO_2/N_2 Responsive Aqueous Foams

R-BMI-C is highly soluble in aqueous solutions at pH 10.4. By bubbling CO_2 into the solution, R-BMI-C was protonated and the pH of the solution was then reduced. In this process, aqueous solutions of R-BMI-C with pH 10.4, 9.2, 8.4, and 7.4 were taken and their foams' properties were explored. As shown in Fig. 10, the initial volume of foams was 7.0, 6.8, 6.6, and 6.2 mL at pH 10.4, 9.2, 8.4 and 7.4, respectively. The initial foams volume decreased slightly with increasing CO_2 content, but the foams' stability increased. The foams half-lives of the aqueous R-BMI-C solutions at pH 10.4, 9.2, 8.4 and 7.4 were 1.5, 13, 37, and 336 h, respectively. The error bars of foaming and foam stabilization tests are shown in Fig. 9. As mentioned above, the foams' stability was related to the structure of the surfactant skeleton, and the rigid structure was more favorable than the flexible chain to stabilize the foams. In addition, the foams' stability is closely related to the foams' particle size. We further observed the foams'

size by fluorescence microscopy and found from Fig. 11 that the foams' particle size decreases with increasing pH. It is well known that the smaller the foams particle size, the stronger the resistance to coarsening process and the stronger the foams' stability [29]. In summary, the foams formed by the aqueous solution of R-BMI-C have excellent CO_2 responsiveness.
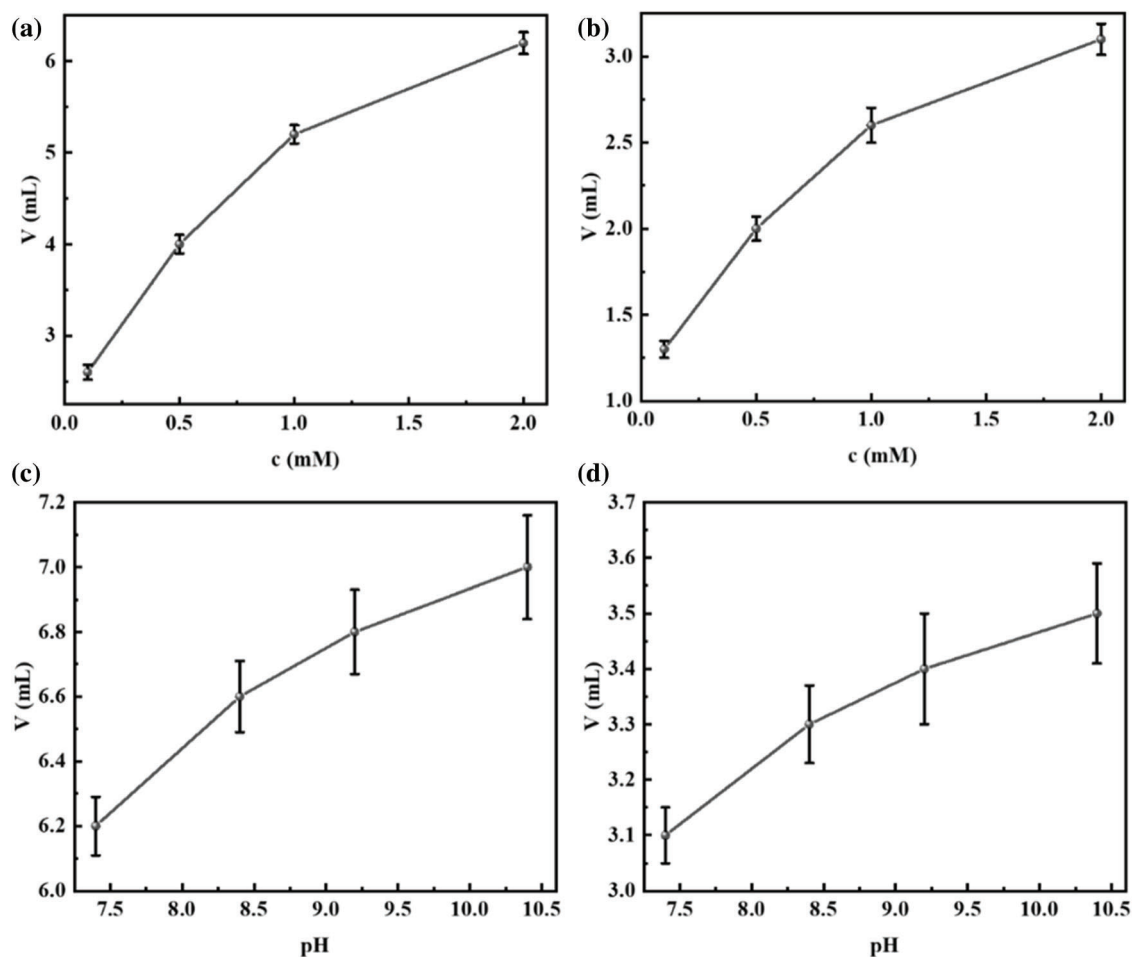

Figure 9: (a) Error bars of foaming tests for different concentrations of R-BMI-C aqueous solution; (b) error bars of foam volume at half-life for R-BMI-C aqueous solutions of different concentrations; (c) error bars of foaming tests for different pH values of R-BMI-C aqueous solution; (d) error bars of foam volume at half-life for R-BMI-C aqueous solutions of different pH values

We also investigated the responsiveness of R-BMI-C (2 mM) aqueous solutions to CO_2/N_2. As shown in Fig. 12, the bubbling CO_2 modulates the pH of the solution to 7.4 and the transmittance is 76.09%. At this time, R-BMI-C aqueous solution could form abundant and stable foams with an initial volume of 6.2 mL and a foams half-life of up to 336 h. At 65°C, N_2 was introduced into the above solution to blow away the CO_2 in the solution. The pH of the solution then rose to 10.4 and the transmittance of the R-BMI-C aqueous solution was close to 100%. At this point, the initial volume of foams formed by R-BMI-C aqueous solution increased to 7 mL, but the foams collapsed completely within 2 h. In addition, continuing to blow CO_2 into the R-BMI-C aqueous solution to adjust the pH to 7.4, stable foams with an initial volume of 6.2 mL could be formed again. The process of changing the foaming and defoaming properties of R-BMI-C aqueous solution by bubbling CO_2/N_2 can be cycled at least three times, indicating that

R-BMI-C aqueous solution has excellent CO_2/N_2 responsiveness. The changes in molecular structure and macroscopic self-assembly before and after the response of R-BMI-C are shown in Fig. 13. By bubbling CO_2 into the R-BMI-C aqueous solution, some of the carboxylate ions of R-BMI-C were protonated to form carboxylic acids. The macroscopic scale shows the transition from a clarified aqueous solution to a turbid state. By bubbling N_2 into the solution, the carboxylic acid in the R-BMI-C molecule is deprotonated back to the initial state.
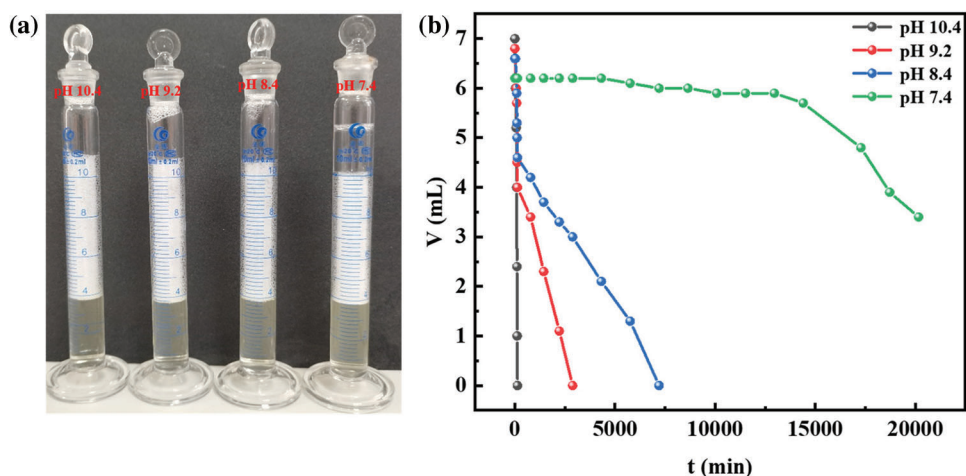

Figure 10: (a) Digital photographs of aqueous foams (b) Variation of foams volume by R-BMI-C aqueous solutions with pH 7.4, 8.4, 9.2 and 10.4 at a concentration of 2 mM
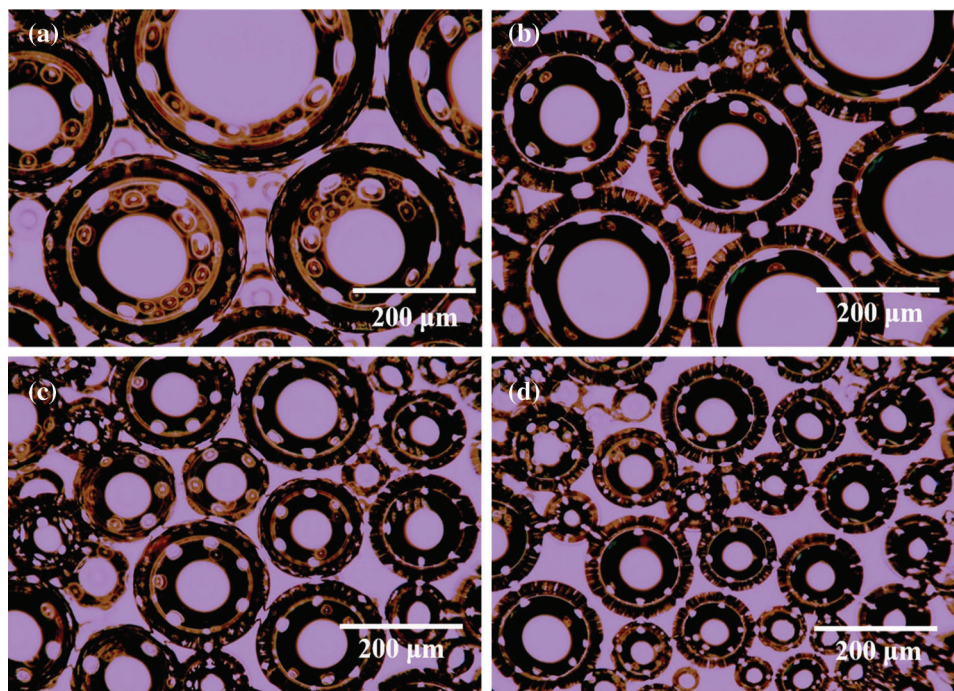

Figure 11: Foam micrographs of foams by R-BMI-C aqueous solutions at (a) pH 10.4, (b) pH 9.2, (c) pH 8.4 and (d) pH 7.4 at a concentration of 2 mM (All foam micrographs were taken at 5 min of foam preparation)
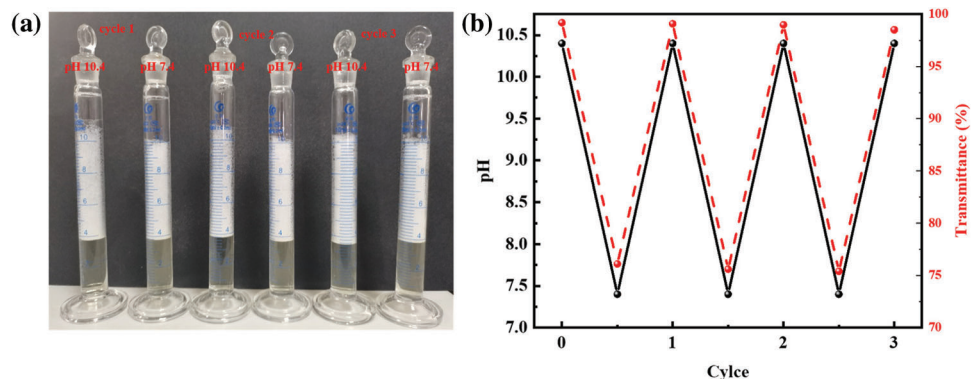
Figure 12: (a) Digital photographs of aqueous foams, (b) pH and transmittance for three responsive of R-BMI-C aqueous solutions at 2 mM
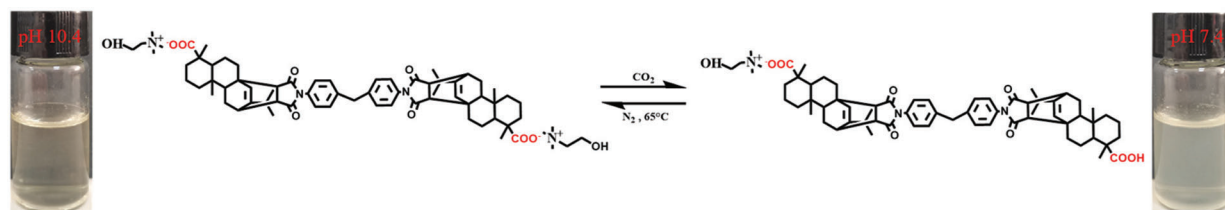

Figure 13: CO_2/N_2-responsive R-BMI-C structural reversible transition; The inset corresponds to the schematic diagram of the CO_2-induced self-assembly transition of R-BMI-C in aqueous solution

3.7 Mechanism of CO_2 Responsive and Photoresponsive Foams

Various properties of surfactants, such as emulsification, solubilization, foaming, and foams stabilization, are closely related to surfactant self-assembled structures [30,31]. The self-assembly morphology can be described by the molecular arrangement parameter $p = v/a_0l$, where v and l are the volume and maximum effective extension length of the hydrophobic group of the surfactant, respectively, and a_0 is the effective area occupied by the hydrophilic group of the surfactant on the surface of the aggregates. When $p < 1/3$, the surfactant tends to form spherical micelles, self-aggregates to form worm micelles at $1/3 < p < 1/2$. For $1/2 < p < 1$, a vesicle structure is formed in solution and obtains a bilayer structure at $p \approx 1$ [32,33]. The self-assembled structure of surfactants depends on the interaction forces between surfactant molecules, including hydrogen bonding, electrostatic interactions, van der Waals forces, and hydrophobic forces. Among them, hydrophobic forces are the key driving force for the aggregation of surfactants to form different aggregates [30,34]. Currently, the most common method to increase the hydrophobic interaction of surfactants is to increase the hydrophobic group of surfactants, thus enhancing surfactant self-assembly [35]. In addition, the electrostatic interaction between the charge ion head groups of surfactants is also an effective means to enhance the intermolecular forces of surfactants. The self-assembled structure of surfactants can be changed by adjusting the composition or concentration of anionic and cationic surfactants.

To investigate the structure of R-BMI-C aqueous solution aggregates, we obtained their internal structure diagrams by Cryo-TEM, as shown in Fig. 14. Before bubbling CO_2, R-BMI-C had strong hydrophobic interactions between the bulky rigid groups and electrostatic interactions between the charge ion head groups. Both interactions lowered the packing parameters and formed spherical micelles in the solution (Fig. 14a at the red arrow). The foams produced by spherical micelles are unstable but the foams produced by laminar or vesicular micelles are extremely stable [15]. The intervention of either CO_2

provides H^+, which protonates some of the carboxyl groups of R-BMI-C. At this point, the electrostatic force between surfactant head groups decreases. When both forms of R-BMI-C protonated and deprotonated coexist, hydrogen bonds can be formed between the molecules of both forms. As a result, the effective headgroup area decreases while the packing parameter increases and R-BMI-C self-assembles to form lamellar micelles (Fig. 14b at the yellow arrow). Fig. 15 shows the transition of the self-assembled microstructure from spherical micelles to lamellar micelles [36]. The lamellar structure tends to adsorb at the air/water interface or is trapped in the foams film. And they avoid the too fast exchange of surfactant molecules at the interface or between monomers. As a result, foams' coarsening and coalescence processes are slowed down, and foams' stability is significantly increased [37].
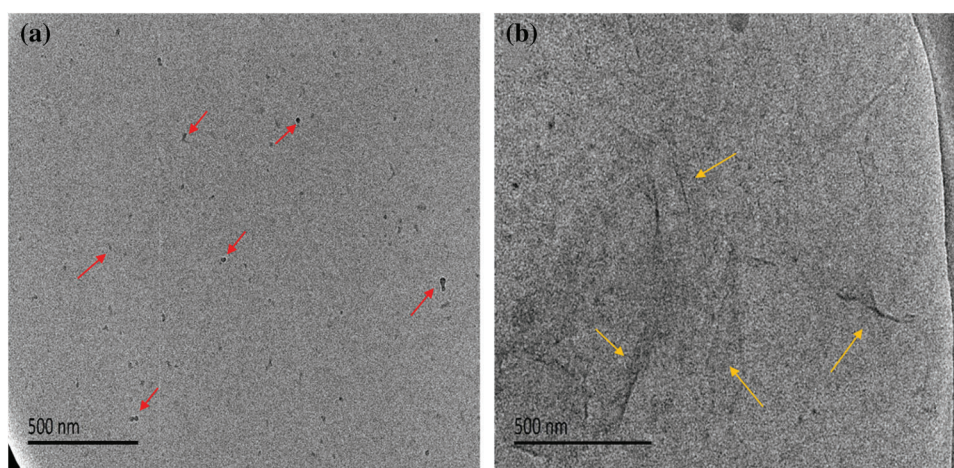

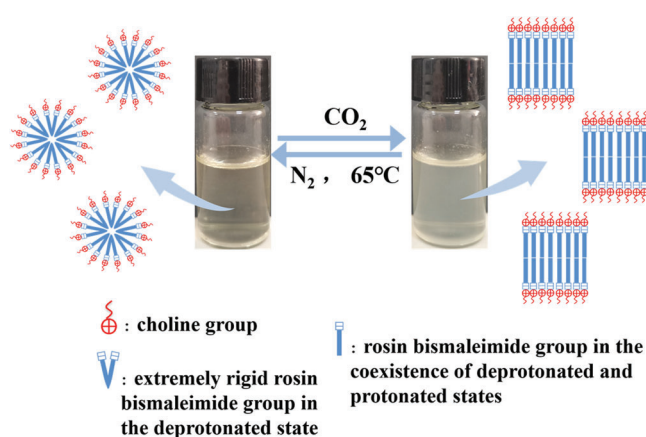**Figure 14:** Cryo-TEM images of R-BMI-C aqueous solution (a) at pH 10.4 and (b) after bubbling CO_2

Figure 15: Schematic diagram of microstructure changes in CO_2 responsive of R-BMI-C aqueous solution

4 Conclusion

Most reported CO_2-responsive surfactants mainly focus on surfactants with straight-chain alkyl groups as lipophilic groups, and responsive surfactants with larger rigid groups have rarely been studied. In this work, the rosin-based surfactant R-BMI-C was synthesized by simply mixing R-BMI with choline hydroxide in a molar ratio of 1:2.4. This process avoided complex synthetic reactions and can reduce the

reaction cost. And the clean response of bio-based surfactant was achieved by using CO_2 as triggering agents. The foams prepared by R-BMI-C at pH 10.4 were unstable with a half-life of only 1.5 h. The foams stability can be enhanced by lowering the pH of the solution by bubbling CO_2. According to the results, the foams prepared at pH 7.4 were exceptionally stable with a half-life of up to 336 h. In addition, unstable foams can be formed again by blowing away CO_2 by bubbling N_2 into the solution. The intervention of CO_2/N_2 enables at least three transitions between stable and unstable foams. The CO_2 content controls the structure change of the surfactant from bola type to conventional type. The coexistence of both protonated and deprotonated forms of R-BMI-C increases the packing parameters to form a bilayer structure and shows excellent foam stabilization. It is shown that the rigid surfactant R-BMI-C has excellent foams performance and responsiveness and could be widely used in oil extraction, fire fighting, or chemical decontamination.

Conflicts of Interest: The authors declare that they have no conflicts of interest to report regarding the present study.

References

1. Calhoun, S. G. K., Chandran Suja, V., Fuller, G. G. (2022). Foaming and antifoaming in non-aqueous liquids. *Current Opinion in Colloid & Interface Science, 57,* 101558–101572. DOI 10.1016/j.cocis.2021.101558.

2. Wang, Z., Ren, G., Yang, J., Xu, Z., Sun, D. (2019). CO_2-responsive aqueous foams stabilized by pseudogemini surfactants. *Journal of Colloid and Interface Science, 536,* 381–388. DOI 10.1016/j.jcis.2018.10.040.

3. Lin, Q., Liu, K. H., Cui, Z. G., Pei, X. M., Jiang, J. Z. et al. (2018). pH-responsive pickering foams stabilized by silica nanoparticles in combination with trace amount of dodecyl dimethyl carboxyl betaine. *Colloids and Surfaces A: Physicochemical and Engineering Aspects, 544,* 44–52. DOI 10.1016/j.colsurfa.2018.02.027.

4. Amani, P., Miller, R., Javadi, A., Firouzi, M. (2022). Pickering foams and parameters influencing their characteristics. *Advanced in Colloid Interface Science, 301,* 102606–102630. DOI 10.1016/j.cis.2022.102606.

5. Raj, S., Krishnan, J. M., Ramamurthy, K. (2022). Influence of admixtures on the characteristics of aqueous foam produced using a synthetic surfactant. *Colloids and Surfaces A: Physicochemical and Engineering Aspects, 643,* 128770–128782. DOI 10.1016/j.colsurfa.2022.128770.

6. Xu, J., Qiao, H., Yu, K., Chen, M., Liu, C. et al. (2022). Cu^{2+} tunable temperature-responsive pickering foams stabilized by poly (N-isopropylacrylamide-co-vinyl imidazole) microgel: Significance for Cu^{2+} recovery via flotation. *Chemical Engineering Journal, 442,* 136274–136290. DOI 10.1016/j.cej.2022.136274.

7. Zhai, Z., Xu, J., Yan, X., Song, Z., Shang, S. et al. (2020). pH-responsive foams based on a transition between a bola surfactant and a traditional surfactant. *Journal of Molecular Liquids, 298,* 111968–111974. DOI 10.1016/j.molliq.2019.111968.

8. Sheng, Y., Yan, C., Li, Y., Peng, Y., Ma, L. et al. (2021). Thermal stability of gel foams stabilized by xanthan gum, silica nanoparticles and surfactants. *Gels, 7(4),* 1–13. DOI 10.3390/gels7040179.

9. Sheng, Y., Xue, M., Zhang, S., Wang, Y., Zhai, X. et al. (2021). Effect of xanthan gum and silica nanoparticles on improving foam properties of mixed solutions of short-chain fluorocarbon and hydrocarbon surfactants. *Chemical Engineering Science, 245,* 116952–116962. DOI 10.1016/j.ces.2021.116952.

10. Wan, Z., Sun, Y., Ma, L., Zhou, F., Guo, J. et al. (2018). Long-lived and thermoresponsive emulsion foams stabilized by self-assembled saponin nanofibrils and fibrillar network. *Langmuir, 34(13),* 3971–3980. DOI 10.1021/acs.langmuir.8b00128.

11. Fan, X., Guan, X., Zhang, M., Liu, Y., Li, Y. (2022). Aqueous foam synergistically stabilized by the composite of lignin nanoparticles and surfactant. *Colloids and Surfaces A: Physicochemical and Engineering Aspects, 643,* 128727–128740. DOI 10.1016/j.colsurfa.2022.128727.

12. Lei, L., Xie, D., Song, B., Jiang, J., Pei, X. et al. (2017). Photoresponsive foams generated by a rigid surfactant derived from dehydroabietic acid. *Langmuir, 33(32),* 7908–7916. DOI 10.1021/acs.langmuir.7b00934.

13. Fameau, A. L., Lam, S., Velev, O. D. (2013). Multi-stimuli responsive foams combining particles and self-assembling fatty acids. *Chemical Science, 4(10),* 8264–8269. DOI 10.1039/c3sc51774h.

14. Sun, S., Zhang, X., Feng, S., Wang, H., Wang, Y. et al. (2019). CO_2/N_2 switchable aqueous foam stabilized by SDS/C_{12}A surfactants: Experimental and molecular simulation studies. *Chemical Engineering Science, 209,* 115218–115226. DOI 10.1016/j.ces.2019.115218.

15. Fameau, A. L., Saint-Jalmes, A., Cousin, F., Houinsou, B., Novales, B. et al. (2011). Smart foams: Switching reversibly between ultrastable and unstable foams. *Angewandte Chemie International Edtion, 50(36),* 8264–8269. DOI 10.1002/anie.201102115.

16. Jochum, F. D., Theato, P. (2013). Temperature-and light-responsive smart polymer materials. *Chemical Society Reviews, 42(17),* 7468–7483. DOI 10.1039/C2CS35191A.

17. Binks, B. P., Murakami, R., Armes, S. P., Fujii, S. (2005). Temperature-induced inversion of nanoparticle-stabilized emulsions. *Angewandte Chemie International Edtion, 44(30),* 4795–4798. DOI 10.1002/(ISSN)1521-3773.

18. Wang, J., Liang, M., Tian, Q., Feng, Y., Yin, H. et al. (2018). CO_2-switchable foams stabilized by a long-chain viscoelastic surfactant. *Journal of Colloid and Interface Science, 523,* 65–74. DOI 10.1016/j.jcis.2018.03.090.

19. Li, C., Wang, Z., Wang, W., Zhu, H., Sun, S. et al. (2022). Temperature and salt resistant CO_2 responsive gas well foam: Experimental and molecular simulation study. *Applied Surface Science, 594,* 153431–153459. DOI 10.1016/j.apsusc.2022.153431.

20. Chen, A., Wang, D., Chen, J., Xu, J., Zeng, H. (2022). A CO_2/N_2-responsive pickering emulsion stabilized by novel switchable surface-active alumina nanoparticles. *Engineering, 12,* 48–54. DOI 10.1016/j.eng.2020.08.031.

21. Schnurbus, M., Stricker, L., Ravoo, B. J., Braunschweig, B. (2018). Smart air-water interfaces with arylazopyrazole surfactants and their role in photoresponsive aqueous foam. *Langmuir, 34(21),* 6028–6035. DOI 10.1021/acs.langmuir.8b00587.

22. Brocas, A. L., Llevot, A., Mantzaridis, C., Cendejas, G., Auvergne, R. et al. (2013). Epoxidized rosin acids as co-precursors for epoxy resins. *Designed Monomers and Polymers, 17(4),* 301–310. DOI 10.1080/15685551.2013.840504.

23. Zhai, Z., Yan, X., Song, Z., Shang, S., Rao, X. (2018). Annular and threadlike wormlike micelles formed by a bio-based surfactant containing an extremely large hydrophobic group. *Soft Matter, 14(4),* 499–507. DOI 10.1039/C7SM02163A.

24. Yan, X., Zhai, Z., Xu, J., Song, Z., Shang, S. et al. (2018). CO_2-responsive pickering emulsions stabilized by a bio-based rigid surfactant with nanosilica. *Jouanal of Agricultural and Food Chemistry, 66(41),* 10769–10776. DOI 10.1021/acs.jafc.8b03458.

25. Chen, J., Song, B., Pei, X., Cui, Z., Xie, D. (2019). Rheological behavior of environmentally friendly viscoelastic solutions formed by a rosin-based anionic surfactant. *Journal of Agricultural and Food Chemistry, 67(7),* 2004–2011. DOI 10.1021/acs.jafc.8b06985.

26. Yan, Y., Xiong, W., Huang, J., Li, Z., Li, X. et al. (2005). Organized assemblies in bolaamphiphile/oppositely charged conventional surfactant mixed systems. *Journal of Physical Chemistry B, 109(1),* 357–364. DOI 10.1021/jp046365d.

27. Han, F., He, X., Huang, J., Li, Z. (2004). Surface properties and aggregates in the mixed systems of bolaamphiphiles and their oppositely charged conventional surfactants. *The Journal of Physical Chemistry B, 108(17),* 5256–5262. DOI 10.1021/jp0497920.

28. Sanchez-Fernandez, A., Moody, G. L., Murfin, L. C., Arnold, T., Jackson, A. J. et al. (2018). Self-assembly and surface behaviour of pure and mixed zwitterionic amphiphiles in a deep eutectic solvent. *Soft Matter, 14(26),* 5525–5536. DOI 10.1039/C8SM00755A.

29. Magrabi, S. A., Dlugogorski, B. Z., Jameson, G. J. (1999). Bubble size distribution and coarsening of aqueous foams. *Chemical Engineering Science, 54(18),* 4007–4022. DOI 10.1016/S0009-2509(99)00098-6.

30. Song, S., Song, A., Hao, J. (2014). Self-assembled structures of amphiphiles regulated via implanting external stimuli. *RSC Advances, 4(79),* 41864–41875. DOI 10.1039/C4RA04849K.

31. Fameau, A. L., Salonen, A. (2014). Effect of particles and aggregated structures on the foam stability and aging. *Comptes Rendus Physique, 15(8–9),* 748–760. DOI 10.1016/j.crhy.2014.09.009.

32. Chu, Z., Dreiss, C. A., Feng, Y. (2013). Smart wormlike micelles. *Chemical Society Reviews, 42(17),* 7174–7203. DOI 10.1039/c3cs35490c.

33. Israelachvili, J. N. (2011). Van der Waals forces between particles and surfaces. *Intermolecular and Surface Forces,* pp. 253–289. USA: Academic Press.

34. Ezrahi, S., Tuval, E., Aserin, A. (2006). Properties, main applications and perspectives of worm micelles. *Advances in Colloid and Interface Science, 128–130,* 77–102. DOI 10.1016/j.cis.2006.11.017.

35. Acharya, D. P., Sato, T., Kaneko, M., Singh, Y., Kunieda, H. (2006). Effect of added poly (oxyethylene)dodecyl ether on the phase and rheological behavior of wormlike micelles in aqueous SDS solutions. *Journal of Physical Chemistry B, 110(2),* 754–760. DOI 10.1021/jp054631x.

36. Arnould, A., Gaillard, C., Fameau, A. L. (2015). pH-responsive fatty acid self-assembly transition induced by UV light. *Journal of Colloid and Interface Science, 458,* 147–154. DOI 10.1016/j.jcis.2015.07.043.

37. Varade, D., Carriere, D., Arriaga, L. R., Fameau, A. L., Rio, E. et al. (2011). On the origin of the stability of foams made from catanionic surfactant mixtures. *Soft Matter, 7(14),* 6557–6570. DOI 10.1039/c1sm05374d.